Electromagnetic forces on a discrete concentrator under time-harmonic illumination

Patrick Chaumet, Sébastien Guenneau

Electromagnetic forces on a discrete concentrator under time-harmonic illumination

Patrick C. Chaumet[1], Sebastien Guenneau[2]
[1] *Institut Fresnel, Aix Marseille Univ, CNRS, Centrale Marseille, Marseille, France*
[2] *UMI 2004 Abraham de Moivre-CNRS, Imperial College London, SW7 2AZ, London, UK*

We study electromagnetic forces and torques experienced on both perfect and discretized transformation-based concentrators, under time-harmonic illumination. The effect of the concentration is investigated in both cases and compared to the case of a perfect cloak. The effect of the dispersion on the optical force and torque is also investigated and the force experienced by a particle located at the center of the concentrator is studied.

PACS numbers: 42.50.Wk,41.20.-q,02.70.-c

Transformation based solutions to the Eikonal equation, when expressed in curvilinear coordinate systems, travel along geodesics rather than in straight lines [1]. Light follows the shortest trajectory, in accordance with the least-time principle formulated by Fermat in 1662. This minimization principle is valid in the ray optics regime, when the wavelength is much smaller than the size of any diffracting object that may be present. Leonhardt showed [2] that this allows one, for instance, to design invisibility cloaks using conformal mappings that simply require a spatially varying refractive index. However, this cloaking mechanism is limited to two-dimensional structures. Pendry, Schurig and Smith simultaneously reported that the same principle can be extended to electromagnetic (EM) waves, *i.e.* when the wavelength is in comparable to the size of the scattering object, by effectively hollowing out a region of space, as far as the EM wave is concerned [3]. This is achieved through spatially varying anisotropic permittivity and permeability tensors. The first practical implementation of the concept of invisibility cloak exploited the properties of concentric rings of split ring-resonators, that generate the required artificial medium at the right microwave frequency [3]. Such a metamaterial cloak effectively maps a concealment region into a surrounding shell thanks to its strongly anisotropic, and spatially varying, effective permittivity and permeability. It also matches the impedance between the device and the surrounding vacuum. The ideal cloak thus neither scatters waves nor does it induce a shadow in the transmitted field. Numerical experiments have shown this remains valid in the near field, when an electromagnetic source is placed in close vicinity, or even within, the cloak [4]. A closely related problem is that of electric impedance tomography [5–7] that aims to uniquely determine the conductivity, within a bounded domain, by applying a known static voltage to the surface and recording the resulting current at the boundary of the domain. Mathematically, this current–voltage relationship provides a Dirichlet-to-Neumann (DtN) map. In order for electric impedance tomography to work, it must be possible to determine the conductivity from a knowledge of the DtN map. If this can be done, then cloaking is impossible. The question of whether or not the DtN map can be used to determine the form of the conductivity is known as the Calderon problem. The singularity and anisotropy of the cloak parameters in [3, 4, 7] and subsequent articles, allow for the possibility that the DtN map does not uniquely determine the conductivity from boundary measurements. Cloaking theory undepinned by DtN map also applies to acoustic [8] and thermal [9, 10] cloaks. Similarly, some Neumann-Poincaré operator unveils the possibility of cloaking via localized anomalous resonances induced by sign-shifting parameters across some cloak's boundaries [11], as first proposed by Milton and Nicorovici in [12]. Such external cloaks can be designed via space folding transforms and allow for a local amplification of the EM field, an effect akin to Schrödinger hats in the context of the Schrödinger equation [13].

While there has been a strong focus on the effects of cloaking devices on the EM fields themselves, electromagnetic forces and torques have not been the object of the same level of scrutiny. Optical manipulation has been extended to a wider range of configurations in the last decade [14]. For instance, the optical manipulation of electrically and magnetically particle is receiving increasing interest [15, 16]. The main reason behind this is that it is now possible to enhance the magnetic response of matter at optical frequencies, owing to metamaterial architectures, or the properties of silicon particle [17, 18]. One of us previously demonstrated that optical force and torque can be tremendously enhanced within a cloak [19]. We also showed that a particle placed inside a cloak can be subject to a significantly reduced radiation pressure, which is consistent with some earlier proposal to cloak sensors [13, 20–22]. This may seem like an obvious consequence of the cloaking mechanism, however, this is not the full story. Quite remarkably, under certain conditions the force on the particle can be stronger than it would be in the absence of the cloak [19].

While invisibility cloaks have been somewhat of a poster child for transformation optics, changing the nature of the transformation that is applied to the electric and magnetic constants can lead to a drastically different class of devices. For instance, transformation optics can yield metamaterials with other functionalities, such as field rotators and concentrators [23, 24]. In the latter case, one can enhance time-averaged total energy density within an inner core.

In this Letter we investigate optical forces and torques

in the presence of transformation based concentrators. We start by recalling some elements of the theory of optical forces and torques acting on heterogeneous anisotropic magneto-dielectric objects. We then introduce the definition of a spherical concentrator that depends upon a magnifying parameter M (with three limit cases $M = 0$, when the concentrator is akin to a perfect cloak, $M = 1$ when the concentrator reduces to vacuum and M almost equal to 2 when the density of optical force is stronger). We then present and discuss numerical results for representative designs of perfect, dispersive and discrete concentrators. Finally, we study the case of a small dielectric sphere at the center of the concentrator, which can be viewed as a counterpart to the problem of cloaking a sensor.

To compute the optical force and torque experienced by the concentrator, we use the discrete dipole approximation (DDA) as it has the advantage of allowing us to mimic the discrete structure of an actual device without having to deal with the specifics of the internal structure of the metamaterial. This way, the concentrator is represented as a discrete collection of scattering elements, with both electric and magnetic polarizabilities. As the method to compute the optical forces and torques on an anisotropic, magneto-dielectric object with the DDA as been described in a previous article, we only present a brief summary of the method used. The object considered is discretized into a set of N polarizable subunits over a cubic lattice with period d [25, 26]. Each subunit is characterized by an electric polarizability tensor $\boldsymbol{\alpha}^{\mathrm{e}}$ and a magnetic polarizability tensor $\boldsymbol{\alpha}^{\mathrm{m}}$ which account for the radiation reaction [27]. Then the electromagnetic field for each subunit can written as [28]:

$$\begin{aligned}\mathbf{E}(\mathbf{r}_i,\omega) &= \mathbf{E}^{\mathrm{inc}}(\mathbf{r}_i,\omega)\\ &+ \sum_{j=1}^{N}\big[\mathbf{T}^{\mathrm{ee}}(\mathbf{r}_i,\mathbf{r}_j,\omega)\boldsymbol{\alpha}^{\mathbf{e}}(\mathbf{r}_j,\omega)\mathbf{E}(\mathbf{r}_j,\omega)\\ &+ \mathbf{T}^{\mathrm{em}}(\mathbf{r}_i,\mathbf{r}_j,\omega)\boldsymbol{\alpha}^{\mathrm{m}}(\mathbf{r}_j,\omega)\mathbf{H}(\mathbf{r}_j,\omega)\big] \quad (1)\\ \mathbf{H}(\mathbf{r}_i,\omega) &= \mathbf{H}^{\mathrm{inc}}(\mathbf{r}_i,\omega)\\ &+ \sum_{j=1}^{N}\big[\mathbf{T}^{\mathrm{me}}(\mathbf{r}_i,\mathbf{r}_j,\omega)\boldsymbol{\alpha}^{\mathrm{e}}(\mathbf{r}_j,\omega)\mathbf{E}(\mathbf{r}_j,\omega)\\ &+ \mathbf{T}^{\mathrm{mm}}(\mathbf{r}_i,\mathbf{r}_j,\omega)\alpha^{\mathrm{m}}(\mathbf{r}_j,\omega)\mathbf{H}(\mathbf{r}_j,\omega)\big], \quad (2)\end{aligned}$$

where $\mathbf{r}_i$ is a vector that points on the subunit i and ω denotes the angular frequency, $\mathbf{T}$ the free-space field susceptibility tensors [29, 30] and $\{\mathbf{E}^{\mathrm{inc}},\mathbf{H}^{\mathrm{inc}}\}$ the incident electromagnetic field. For the sake of brevity we will omit the dependence on ω henceforth. Equation represents a linear system with $6N$ unknown solved iteratively [31] with FFT techniques [32]. The spatial derivatives of the fields are obtained through [33]:

$$\begin{aligned}\boldsymbol{\nabla}\mathbf{E}(\mathbf{r}_i) &= \boldsymbol{\nabla}\mathbf{E}^{\mathrm{inc}}(\mathbf{r}_i)+\sum_{j=1}^{N}\big[\boldsymbol{\nabla}\mathbf{T}^{\mathrm{ee}}(\mathbf{r}_i,\mathbf{r}_j)\boldsymbol{\alpha}^{\mathrm{e}}(\mathbf{r}_j)\mathbf{E}(\mathbf{r}_j)\\ &+ \boldsymbol{\nabla}\mathbf{T}^{\mathrm{em}}(\mathbf{r}_i,\mathbf{r}_j)\boldsymbol{\alpha}^{\mathrm{m}}(\mathbf{r}_j)\mathbf{H}(\mathbf{r}_j)\big], \quad (3)\\ \boldsymbol{\nabla}\mathbf{H}(\mathbf{r}_i) &= \boldsymbol{\nabla}\mathbf{H}^{\mathrm{inc}}(\mathbf{r}_i)+\sum_{j=1}^{N}\big[\boldsymbol{\nabla}\mathbf{T}^{\mathrm{me}}(\mathbf{r}_i,\mathbf{r}_j)\boldsymbol{\alpha}^{\mathrm{e}}(\mathbf{r}_i)\mathbf{E}(\mathbf{r}_i)\\ &+ \boldsymbol{\nabla}\mathbf{T}^{\mathrm{mm}}(\mathbf{r}_i,\mathbf{r}_j)\boldsymbol{\alpha}^{\mathrm{m}}(\mathbf{r}_j)\mathbf{H}(\mathbf{r}_j)\big]. \quad (4)\end{aligned}$$

Hence the optical force and torque are deduced from [29]:

$$\begin{aligned}F^k(\mathbf{r}_i) &= \frac{1}{2}\mathrm{Re}\Big\{p^l(\mathbf{r}_i)\partial^k\left[E^l(\mathbf{r}_i)\right]^* + m^l\partial^k\left[H^l(\mathbf{r}_i)\right]^*\\ &- \frac{2k^4}{3}\epsilon^{kln}p^l(\mathbf{r}_i)\left[m^n(\mathbf{r}_i)\right]^*\Big\}, \quad (5)\\ \boldsymbol{\Gamma}(\mathbf{r}_i) &= \mathbf{r}_i\times\mathbf{F}(\mathbf{r}_i)\\ &+ \frac{1}{2}\mathrm{Re}\Big\{\mathbf{p}(\mathbf{r}_i)\times\left[\mathbf{E}(\mathbf{r}_i)+\frac{2}{3}ik_0^3\mathbf{p}(\mathbf{r}_i)\right]^*\\ &+ \mathbf{m}(\mathbf{r}_i)\times\left[\mathbf{H}(\mathbf{r}_i)+\frac{2}{3}ik_0^3\mathbf{m}(\mathbf{r}_i)\right]^*\Big\}, \quad (6)\end{aligned}$$

where k_0 is the wavenumber in vacuum, $\times$ denotes the cross-product, ϵ^{kln} is the Levi-Civita tensor, k, l or n stands for either x, y or z, and * denotes the complex conjugate of a complex variable. We note the presence for the optical force of a term proportional to the cross product of the electric and magnetic dipoles, which is required to satisfy the optical theorem [29, 34–36].

It is by now well known (cf. [23] and subsequent works) that a spherical concentrator $\mathcal{B}_a$ of outer radius $r = a$, consisting of an anisotropic heterogeneous shell $\{b \le r \le a\}$ and of an isotropic homogeneous inner core $\mathcal{B}_b = \{0 \le r \le b\}$ can be deduced from a first radial function f that maps $\mathcal{B}_b$ onto another spherical region $\mathcal{B}_{bM} = \{0 \le r' \le bM\}$ $(0 \le M)$ using a linear function

$$r = f(r') = \frac{r'}{M} \text{ for } 0 \le r' \le bM \quad (7)$$

where M is such that $f(0) = 0$ and $f(bM) = b$. Correspondingly, a second radial function h maps a shell $\mathcal{B}_a \setminus \mathcal{B}_b = \{b \le r \le a\}$ on another shell $\mathcal{B}_a \setminus \mathcal{B}_{bM} = \{bM \le r' \le a\}$:

$$r = h(r') = \frac{a - bM}{a - b} + gr' \text{ for } bM \le r' \le a \quad (8)$$

where g is such that $h(bM) = b$ and $h(a) = a$.

The relative permittivity and permeability tensors inside the concentrator are defined in $\mathcal{B}_b$ as:

$$\boldsymbol{\mu} = \boldsymbol{\varepsilon} = M\mathbf{I} \quad (9)$$

with $\mathbf{I}$ the 3×3 identity matrix. In the shell $\mathcal{B}_b \setminus \mathcal{B}_a$ we have:

$$\boldsymbol{\mu} = \boldsymbol{\varepsilon} = \left(\mathbf{I} + \frac{\mathbf{r}\otimes\mathbf{r}}{r^4}g\,(g-2r)\right)\frac{a-bM}{a-b} \quad (10)$$

$$\text{with } g = \frac{ab(1-M)}{(a-bM)}, \quad (11)$$

where $\otimes$ denotes the tensor product. The salient consequence is that the concentrator magnifies by a factor M the incident field in its core $\mathcal{B}_b$. We further note that since $\mu = \varepsilon$, the concentrator is impedance matched to vacuum everywhere in $\mathcal{B}_b$, so it does not reflect any incoming wave (it is transparent). For the DDA the relationship between the electric and magnetic polarizabilities of the subunit used in Eqs (1) and (2) and the relative permittivities and permeabilities of the object, respectively, reads:

$$\boldsymbol{\alpha}^{\mathrm{e}}(\mathbf{r}_j) = \boldsymbol{\alpha}_0^{\mathrm{e}}(\mathbf{r}_j)\left[\mathbf{I} - \frac{2}{3} i k_0^3 \boldsymbol{\alpha}_0^{\mathrm{e}}(\mathbf{r}_j)\right]^{-1} \quad (12)$$

$$\boldsymbol{\alpha}_0^{\mathrm{e}}(\mathbf{r}_j) = \frac{3d^3}{4\pi}\left(\boldsymbol{\varepsilon}(\mathbf{r}_j) - \mathbf{I}\right)\left(\boldsymbol{\varepsilon}(\mathbf{r}_j) + 2\mathbf{I}\right)^{-1} \quad (13)$$

$$\boldsymbol{\alpha}^{\mathrm{m}}(\mathbf{r}_j) = \boldsymbol{\alpha}_0^{\mathrm{m}}(\mathbf{r}_j)\left[\mathbf{I} - \frac{2}{3} i k_0^3 \boldsymbol{\alpha}_0^{\mathrm{m}}(\mathbf{r}_j)\right]^{-1} \quad (14)$$

$$\boldsymbol{\alpha}_0^{\mathrm{m}}(\mathbf{r}_j) = \frac{3d^3}{4\pi}\left(\boldsymbol{\mu}(\mathbf{r}_j) - \mathbf{I}\right)\left(\boldsymbol{\mu}(\mathbf{r}_j) + 2\mathbf{I}\right)^{-1} \quad (15)$$

for $j = 1, \cdots, N$. $\boldsymbol{\alpha}_0$ is the polarizability for the small subunit in using the Clausius-Mossotti relationship for electric or magnetic dipole and $\boldsymbol{\alpha}$ is the polarizability in taking into account the radiative reaction term [27].

Throughout this Letter, we assume the cloak is illuminated by a plane wave with circular polarization, travelling in the positive z direction, with an irradiance 12 μW/μm^2. Units for optical forces and torques are Newtons and Newton meters, respectively and the wavelength is in the visible range, $\lambda_0 = 600$ nm. A sketch of the configuration is given in Fig. 1.

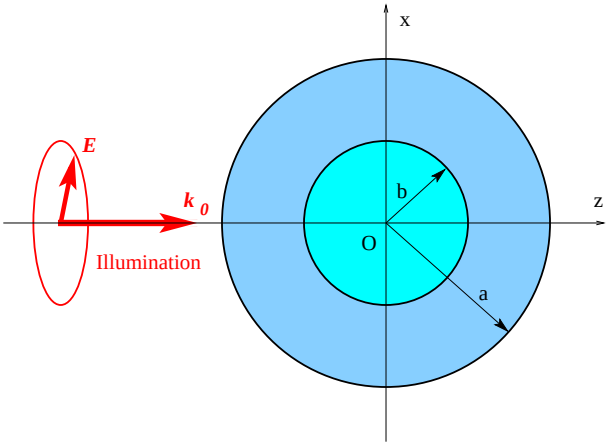

FIG. 1: A concentrator with an outer radius a and an inner core b. The illumination is done with a plane wave with a wave vector $\mathbf{k}_0$ along the z direction and a circular polarization.

A perfect concentrator experiences no net optical force or torque, but inside this one, particularly in the shell where the electromagnetic field undergoes strong variations, there is a density of optical force and optical torque. Figure 2 presents the computation of a concentrator with parameter $a = 2b = \lambda/2$. The density of energy (first row) the density of optical force (second row) and the density of optical torque (x! row). The small bar in the subfigures indicates the scale for the force or torque density.

The case $M = 0$ looks similar to an optical cloak, *i.e.*, there is no field inside the concentrator and no scattering outside the concentrator, as shown by the density of energy equal to zero for $r < b$ and the density of energy constant for $r > a$, see Fig. 2(a). Notice that for $M = 1$ there is no concentrator, the medium is simply vacuum, hence when M gets closer to 1 the densities of optical force and torque decrease, that is why the values of the densities are weaker for the case $M = 0.5$. For $M = 1.5$ we can see the density of energy at the center of the cloak ($r < b$) is constant and stronger than the density of energy outside the cloak. This is the effect for the concentrator for $M > 1$, see Fig. 2(a). Nevertheless, the magnitude of the densities of optical force and torque is of the same order as for the concentrator with $M = 0$, but the maxima are located close to the boundary $r = b$, which implies an important stress between the core ($r < b$) and the outer shell of the concentrator. When $M = 1.9$ the density of energy inside the core ($r < b$) is clearly stronger than in the case $M = 1.5$, see Fig. 2(d). The consequence, is that the density of optical force is stronger than for any other value of M, and it is confined very near the inner boundary $r = b$. For $M = 2$, g is not defined, and therefore the forces and torques cannot be computed. Values above $M = 2$ cannot be computed as the matrix is ill conditioned and all the iterative methods tested fail [31]. Notice that the density of optical force always vanishes at the center of the concentrator, which can be easily understood as the density of energy is constant as we have a plane wave. But in the case where $M = 1.9$, we can see close to the edge for $r < b$ a force density appearing, see Fig. 2(h). This is because the cloak is represented by a discrete structure with the DDA and therefore does not correspond to a perfect cape. The density of optical torque has the same behaviour than the density of optical force. All these features can be understood as the light being "bent" more strongly when M is far from 1 and particularly when M is close to 2. This effect can be maximized when b is closer to a (not shown), as when the width of the outer shell decreases the spatial variation of the field increases.

Of course, there is no net optical force and torque ex-

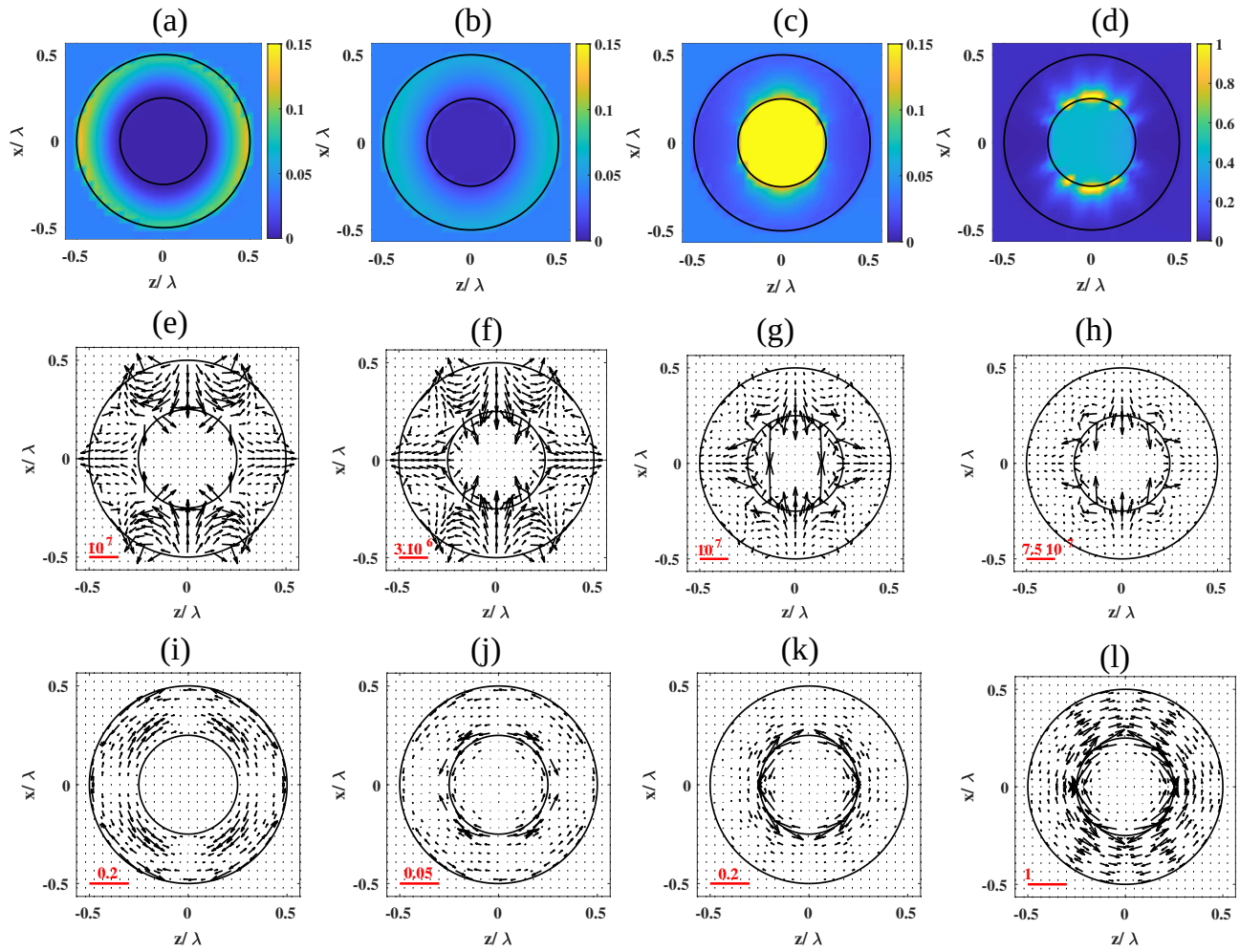

FIG. 2: The concentrator has the dimension $a = \lambda/2$, $b = a/2$ and $N_l = 23$ with $M = 0$ for the first column: (a,e,i); $M = 0.5$ for the second column: (b,f,j); $M = 1.5$ for the third column: (c,g,k); $M = 1.9$ for the fourth column: (d,h,l). In the first line the density of energy is represented in color scale. In the second line the density of the optical force and in the third line the density of the optical torque. The red bar represents the scale with the multiplicative factor.

perienced by a lossless and perfect concentrator, but as underlined by the Kramers-Kronig relation we have always dispersion (we refer to [37] for theoretical bounds on passive cloaking). We can introduce dispersion into our problem by multiplying the relative permittivity and permeability by a factor $f(\omega)$ such that:

$$f(\omega) = f_\infty - \frac{F}{\omega^2 + i\Gamma\omega - \omega_g^2}. \tag{16}$$

We use $\omega_g = \omega_0/10$ and $\Gamma = 0.01$. In Fig. 3 we plot the net optical force experienced by the concentrator versus the wavelength. We have a weak sensitivity of the optical force to the values M irrespective of the wavelength used. In fact the net force on the concentrator is more or less the optical force experienced by an homogeneous sphere of permittivity and permeability $f(\omega)$. We can notice that the concentror at $M = 0$ is not behaving exactly like an optical cloak. It comes from the fact that in the presence of dispersion, light seeps to the center of the structure, and whereas for a cloak we have $\varepsilon = \mu = \mathbf{I}$, for the concentrator we have $\varepsilon = \mu = \mathbf{0}$. The same observation holds for the net optical torque, except that the torque exhibits larger variations when M is close to 2.

The optical force and torque experienced by a perfect concentrator should be zero. However, in practice, a concentrator would be constructed from metamaterials, which are generally made up of a lattice of split-ring resonators. Hence, in our computational model, each element of the DDA can be seen as an element of metamaterial, endowed with both an electric and magnetic response. Using the DDA approach, we can study the influence of the lattice spacing on the forces and torques. The first consequence is that the net force experienced by the concentrator is slightly positive, obviously this force decreases when the lattice spacing as shown in Fig. 4(a) in solid line. However, we can see that the force on the core of the concentrator (Force ins) is almost the

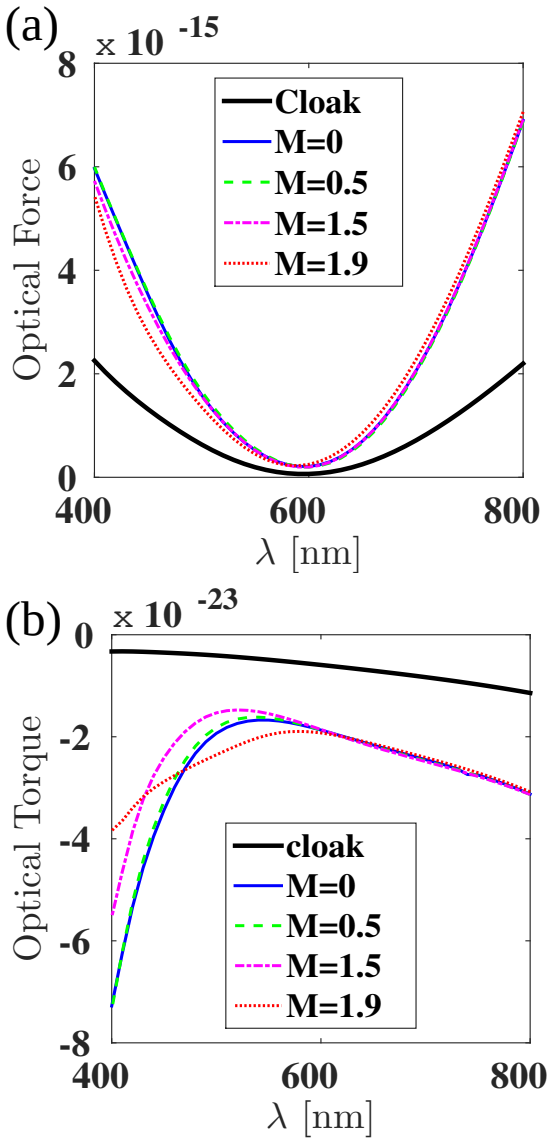

FIG. 3: $a = \lambda/2$, $b = a/2$ and $N_l = 23$. (a) Force experienced on the concentrator for different value of M versus the wavelength of illumination. (b) Optical torque experienced on the concentrator for different value of M versus the wavelength of illumination.

opposite of that experienced by the outer shell (Force ext). These two opposite optical forces show that the concentrator is under mechanical stress, and this stress becomes particularly strong when the number of layer (N_l) decreases.Hence, to decrease the stress inside the concentrator, we have to increase the number of split-ring resonators. For the optical torque, we get the same behaviour except that the net optical torque is equal to zero. This is due to the symmetry of the concentrator and the lack of material losses [38]. If we add loss to this discrete concentrator, as we get the optical force experienced by an homogeneous sphere of permittivity and permeability $f(\omega)$, the effect of the discretization vanishes, as the optical force due to the effect of this discretization is weak compare to the net optical force due to the introduction of the absorbing part with $f(\omega)$.

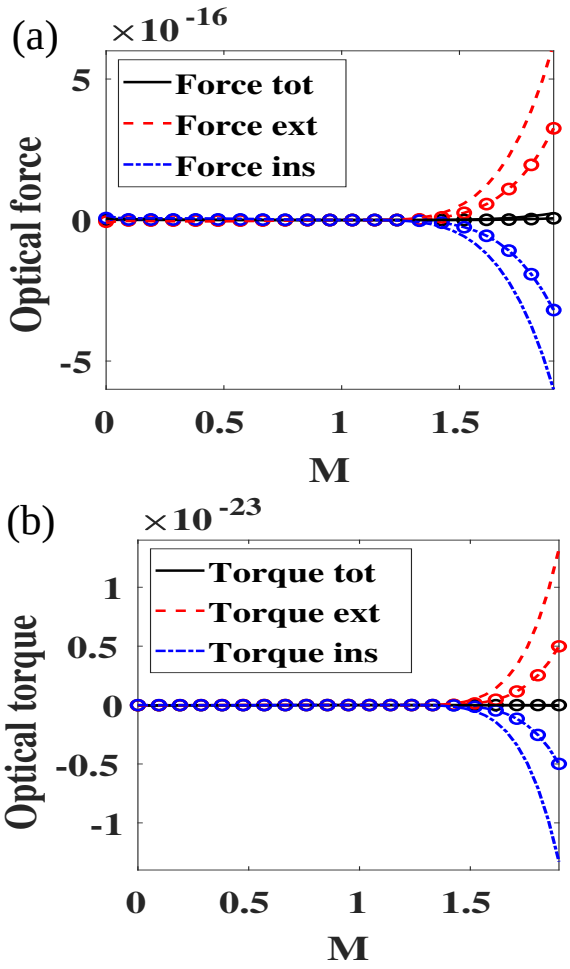

FIG. 4: $a = \lambda/2$, $b = a/2$ and $N_l = 23$ without symbol and $N_l = 32$ with o symbols. (Upper panel) Optical force. (Lower panel) Optical torque.

We now place a small dielectric sphere at the center of the concentrator. To do this, the polarizability of the subunit located at the origin is computed with Eqs. (13) and (15) with $\varepsilon = 2.25$ and $\mu = 1$ which corresponds to a minute sphere in glass with a radius $\left(\frac{3}{4\pi}\right)^{1/3} d$. Being non-magnetic, the sphere only experiences an electric optical force. When $M = 1$ the dipole is in vacuum. Of course, in that case there is no gradient force on the dipole and it only experiences the radiation pressure. In Fig. 5(a) we plot the force experienced by the particle versus M normalized to the optical force exerted on the particle in free space. The optical force on an electric particle can be written as $\mathbf{F} = \frac{1}{2}\mathrm{Re}\left(\alpha E_i \boldsymbol{\nabla} E_i^*\right)$ and this force can be shared into three parts as:

$$\begin{aligned}\mathbf{F} &= \frac{1}{4}\mathrm{Re}(\alpha)\boldsymbol{\nabla}|\mathbf{E}|^2 + \frac{1}{2}k_0\mathrm{Im}(\alpha)\mathrm{Re}\left(\mathbf{E}^* \times \mathbf{H}\right) \\ &- \frac{1}{2}k_0\mathrm{Im}(\alpha)\mathrm{Re}\left[i(\mathbf{E}^*.\boldsymbol{\nabla})\mathbf{E}\right]. \qquad (17)\end{aligned}$$

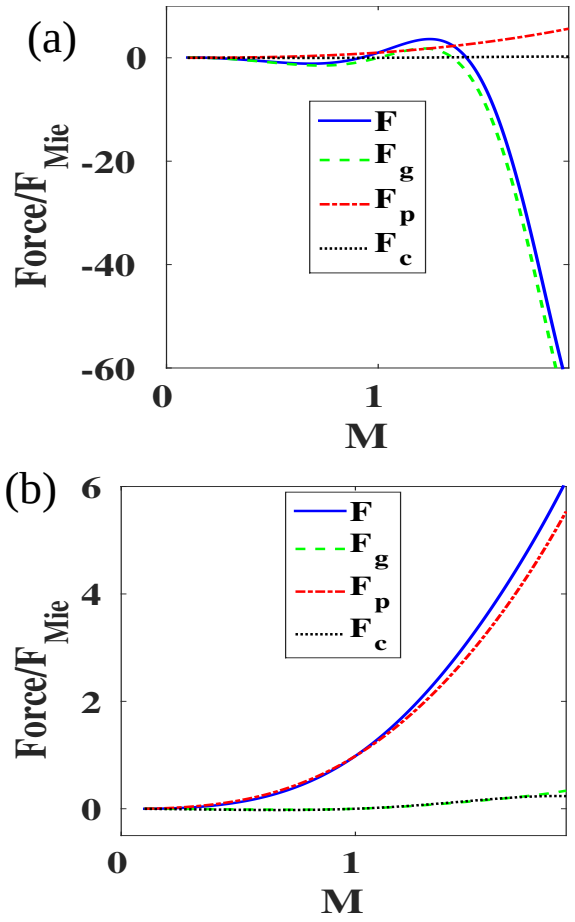

FIG. 5: $a = \lambda/2$, $b = a/2$ and $N_l = 23$. Optical force experienced by a dipole located at the center of the concentrator versus M. This force is normalized by the optical force experienced by the same dipole in free space. (a) $\varepsilon = 2.25$. (b) $\varepsilon = 2.25 + i$.

The first term represents the gradient force ($\mathbf{F}_g$), the second term is related to the radiation pressure, and is proportional to the Poynting vector ($\mathbf{F}_p$), and the third term ($\mathbf{F}_c$) represents a force associated to the nonuniform distribution of the spin density of light [36, 39, 40]. When the small particle is lossless, Fig. 5(a), the force due to radiation pressure increases versus M, as the density of energy increases with M^2. However, this part remains small compared to the gradient force, particularly when M increases. This is due to the fact that, for a lossless particle, the gradient force is proportional to the third power of the radius whereas the radiation pressure is proportional to the sixth power of the radius [41] and that there is small variation of the intensity of the field inside the discrete concentrator. Notice that the gradient force becomes strongly negative meaning that the slope of the intensity of the field is negative at the center of the concentrator for high values of M. When an absorbing particle is located at the center of the concentrator, *i.e.* $\varepsilon = 2.25 + i$ and $\mu = 1$ in Eqs. (13) and (15), the gradient force becomes small compared to the radiation pressure when M increases, see Fig. 5(b). The concentrator increases the density of energy and therefore the radiation pressure. Notice that the behaviour of the gradient force is different between the two cases (lossless vs absorbing particle). This is due to the fact that in the case of the absorbing particle the interaction between the particle and the concentrator is stronger, and if changes the distribution of the field intensity inside the concentrator. Notice also that the third contribution to the force (due the spin density of light) has the same order of magnitude as the gradient force. This term, just like the gradient force, would vanish for an incident plane wave.

We have studied the influence of the discretization of a spherical concentrator, as well as adding dispersion and the effect of placing a small dielectric sphere in its center on the optical force and torque therein. We believe that enhancing or suppressing optical force and torque at will thanks to a tuning parameter M, which is associated with the concentrator design, can help manipulate small objects with light, without perturbing an ambient electromagnetic field, which is one step further than cloaking a sensor. Since one can discretize surfaces and volumes with elementary bricks for sound control in acoustic metamaterials [42, 43], and as enhanced acoustic pressure sensors is of current interest [44], we hope our work will also foster numerical studies of acoustic radiation forces and torques on perfect and discretized concentrators.

[1] D. Schurig, J. B. Pendry, and D. R. Smith, Opt. Express **14**, 9794 (2006).
[2] U. Leonhardt, Science **312**, 1777 (2006).
[3] D. Schurig, J. J. Mock, B. J. Justice, S. A. Cummer, J. B. Pendry, A. F. Starr, and D. R. Smith, Science **314**, 977 (2006).
[4] F. Zolla, S. Guenneau, A. Nicolet, and J. B. Pendry, Opt. Lett. **32**, 1069 (2007).
[5] A. Greenleaf, M. Lassas, and G. Uhlmann, arXiv preprint math/0302258 (2003).
[6] A. Greenleaf, M. Lassas, and G. Uhlmann, Physiological measurement **24**, 413 (2003).
[7] R. V. Kohn, H. Shen, M. S. Vogelius, and M. I. Weinstein, Inverse Problems **24**, 015016 (2008).
[8] A. N. Norris, Proceedings of the Royal Society A: Mathematical, Physical and Engineering Sciences **464**, 2411 (2008).
[9] R. Schittny, M. Kadic, S. Guenneau, and M. Wegener, Physical review letters **110**, 195901 (2013).
[10] R. V. Craster, S. Guenneau, H. Hutridurga, and G. A. Pavliotis, Multiscale Modeling & Simulation **16**, 1146 (2018).
[11] H. Ammari, G. Ciraolo, H. Kang, H. Lee, and G. W. Milton, Archive for Rational Mechanics and Analysis **208**,

667 (2013).
[12] G. W. Milton and N.-A. P. Nicorovici, Proceedings of the Royal Society A: Mathematical, Physical and Engineering Sciences **462**, 3027 (2006).
[13] A. Greenleaf, Y. Kurylev, M. Lassas, U. Leonhardt, and G. Uhlmann, Proceedings of the National Academy of Sciences **109**, 10169 (2012).
[14] D. Gao, W. Ding, M. Nieto-Vesperinas, X. Ding, M. Rahman, T. Zhang, C. Lim, and C.-W. Qiu, Light Sci Appl. **6**, e17039 (2017).
[15] R. Li, R. Yang, C. Ding, and F. Mitri, Journal of Quantitative Spectroscopy and Radiative Transfer **191**, 96 (2017), ISSN 0022-4073, URL http://www.sciencedirect.com/science/article/pii/S0022407317300456.
[16] F. Mitri, R. Li, R. Yang, L. Guo, and C. Ding, Journal of Quantitative Spectroscopy and Radiative Transfer **184**, 360 (2016), ISSN 0022-4073, URL http://www.sciencedirect.com/science/article/pii/S0022407316302904.
[17] I. nigo Liberal, I. nigo Ederra, R. Gonzalo, and R. W. Ziolkowski, Opt. Express **22**, 8640 (2014), URL http://www.opticsexpress.org/abstract.cfm?URI=oe-22-7-8640.
[18] H. Liu, M. Panmai, Y. Peng, and S. Lan, Opt. Express **25**, 12357 (2017), URL http://www.opticsexpress.org/abstract.cfm?URI=oe-25-11-12357.
[19] P. C. Chaumet, A. Rahmani, F. Zolla, and A. Nicolet, Phys. Rev. E **85**, 143101 (2012).
[20] A. Alù and N. Engheta, Phys. Rev. Lett. **102**, 233901 (2009), URL https://link.aps.org/doi/10.1103/PhysRevLett.102.233901.
[21] A. Greenleaf, Y. Kurylev, M. Lassas, and G. Uhlmann, Physical Review E **83**, 016603 (2011).
[22] X. Chen and G. Uhlmann, Optics express **19**, 20518 (2011).
[23] M. Rahm, D. Schurig, D. A. Roberts, S. A. Cummer, D. R. Smith, and J. B. Pendry, Photonics and Nanostructures - Fundamentals and Applications **6**, 87 (2008), ISSN 1569-4410, the Seventh International Symposium on Photonic and Electromagnetic Crystal Structures, URL http://www.sciencedirect.com/science/article/pii/S1569441007000375.
[24] W. Wang, L. Lin, J. Ma, C. Wang, J. Cui, C. Du, and X. Luo, Opt. Express **16**, 11431 (2008), URL http://www.opticsexpress.org/abstract.cfm?URI=oe-16-15-11431.
[25] P. C. Chaumet, A. Sentenac, and A. Rahmani, Phys. Rev. E **70**, 036606 (2004).
[26] P. C. Chaumet and A. Rahmani, J. Quant. Spect. Rad. Transf. **110**, 22 (2009).
[27] B. T. Draine, Astrophys. J. **333**, 848 (1988).
[28] P. C. Chaumet, Mathematics **10** (2022), ISSN 2227-7390, URL https://www.mdpi.com/2227-7390/10/17/3049.
[29] P. C. Chaumet and A. Rahmani, Opt. Exp. **17**, 2224 (2009).
[30] J. D. Jackson, *Classical Electrodynamics* (Wiley, 1975), 2nd ed.
[31] P. C. Chaumet and A. Rahmani, Opt. Lett. **34**, 917 (2009).
[32] J. J. Goodman and P. J. Flatau, Opt. Lett. **16**, 1198 (2002).
[33] P. C. Chaumet, A. Rahmani, A. Sentenac, and G. W. Bryant, Phys. Rev. E **72**, 046708 (2005).
[34] M. Nieto-Vesperinas and J. J. Saenz, Opt. Lett. **35**, 4078 (2010).
[35] M. Nieto-Vesperinas, J. J. Sáenz, R. Gómez-Medina, and L. Chantada, Opt. Express **18**, 11428 (2010), URL http://www.opticsexpress.org/abstract.cfm?URI=oe-18-11-11428.
[36] R. Gómez-Medina, M. Nieto-Vesperinas, and J. J. Sáenz, Phys. Rev. A **83**, 033825 (2011).
[37] M. Cassier and G. W. Milton, Journal of Mathematical Physics **58**, 071504 (2017).
[38] P. C. Waterman, Phys. Rev. D **3**, 825 (1971).
[39] J. R. Arias-González and M. Nieto-Vesperinas, J. Opt. Soc. Am. A **20**, 1201 (2003), URL http://josaa.osa.org/abstract.cfm?URI=josaa-20-7-1201.
[40] S. Albaladejo, M. I. Marqués, M. Laroche, and J. J. Sáenz, Phys. Rev. Lett. **102**, 113602 (2009), URL https://link.aps.org/doi/10.1103/PhysRevLett.102.113602.
[41] P. C. Chaumet, A. Rahmani, and M. Nieto-Vesperinas, Phys. Rev. B **71**, 045425 (2005).
[42] S. A. Cummer, J. Christensen, and A. Alù, Nature Reviews Materials **1**, 1 (2016).
[43] G. Memoli, M. Caleap, M. Asakawa, D. R. Sahoo, B. W. Drinkwater, and S. Subramanian, Nature communications **8**, 1 (2017).
[44] M. Farhat, W. W. Ahmad, A. Khelif, K. N. Salama, and Y. Wu, Journal of Applied Physics **129**, 104902 (2021).